Princeton Plasma Physics Laboratory

PPPL-5391

Constructing current singularity in a 3D line-tied plasma

Y. Zhou, Y-M. Huang, H. Qin, and A. Bhattacharjee

May 2017

Prepared for the U.S.Department of Energy under Contract DE-AC02-09CH11466.

Constructing current singularity in a 3D line-tied plasma

Yao Zhou,[1,*] Yi-Min Huang,[1] Hong Qin,[1,2] and A. Bhattacharjee[1]
[1]*Department of Astrophysical Sciences and Plasma Physics Laboratory, Princeton University, Princeton, New Jersey 08543, USA*
[2]*Department of Modern Physics, University of Science and Technology of China, Hefei, Anhui 230026, China*

We revisit Parker's conjecture of current singularity formation in 3D line-tied plasmas, using a recently developed numerical method, variational integration for ideal magnetohydrodynamics in Lagrangian labeling. With the frozen-in equation built-in, the method is free of artificial reconnection, hence arguably an optimal tool for studying current singularity formation. Using this method, the formation of current singularity has previously been confirmed in the Hahm-Kulsrud-Taylor problem in 2D. In this paper, we extend this problem to 3D line-tied geometry. The linear solution, which is singular in 2D, is found to be smooth for all system lengths. However, with finite amplitude, the linear solution can become pathological when the system is sufficiently long. The nonlinear solutions turn out to be smooth for short systems. Nonetheless, the scaling of peak current density vs. system length suggests that the nonlinear solution may become singular at a finite length. With the results in hand, we can neither confirm nor rule out this possibility conclusively, since we cannot obtain solutions with system length near the extrapolated critical value.

I. INTRODUCTION.

A long-standing problem in solar physics is why the solar corona, a nearly perfectly conducting plasma where the Lundquist number S can be as high as 10^{14}, has an anomalously high temperature that conventional Ohmic heating cannot explain. Decades ago, Parker (1972) proposed that convective motions in the photosphere will induce current singularities in the corona, and the subsequent magnetic reconnection events can account for substantial heating. This conjecture has remained controversial to this day (Antiochos, 1987; Bogoyavlenskij, 2000; Candelaresi et al., 2015; Craig & Pontin, 2014; Craig & Sneyd, 2005; Janse et al., 2010; Longbottom et al., 1998; Longcope & Strauss, 1994b; Low, 2006, 2010; Ng & Bhattacharjee, 1998; Parker, 1983, 1994; Pontin et al., 2016; Pontin & Hornig, 2015; Rappazzo & Parker, 2013; Rosner & Knobloch, 1982; Tsinganos et al., 1984; van Ballegooijen, 1985, 1988; Wilmot-Smith et al., 2009a,b; Zweibel & Boozer, 1985; Zweibel & Li, 1987).

This controversy fits into the larger context of current singularity formation, which is also a problem of interest in toroidal fusion plasmas (Grad, 1967; Hahm & Kulsrud, 1985; Loizu et al., 2015; Rosenbluth et al., 1973). However, the solar corona, where magnetic field lines are anchored in the photosphere, is often modeled with the so-called line-tied geometry. This is a crucial difference from toroidal fusion plasmas where closed field lines can exist. For clarification, in this article, we refer to the problem of whether current singularities can emerge in 3D line-tied geometry as *the Parker problem*.

Although this problem is inherently dynamical, it is usually treated by examining magnetostatic equilibria for simplicity, as Parker did in the first place. The justification is, if the final equilibrium that an initially smooth magnetic field relaxes to contains current singularities, they must have formed during the relaxation. Here the plasma is supposed to be perfectly conducting, so the equilibrium needs to preserve the magnetic topology of the initial field. Analytically, this topological constraint is difficult to explicitly attach to the magnetostatic equilibrium equation. Numerically, most standard methods for ideal magnetohydrodynamics (MHD) are susceptible to artificial field line reconnection in the presence of (nearly) singular current densities. Either way, to enforce this topological constraint is a major challenge for studying the Parker problem.

It turns out one can overcome this difficulty by adopting Lagrangian labeling, where the frozen-in equation is built into the equilibrium equation, instead of the commonly used Eulerian labeling. Zweibel & Li (1987) first noticed that this makes the mathematical formulation of the Parker problem explicit and well-posed. Moreover, not solving the frozen-in equation numerically avoids the accompanying error and resultant artificial reconnection. A Lagrangian relaxation scheme with this feature has been developed using conventional finite difference (Craig & Sneyd, 1986), and extensively used to study the Parker problem (Craig & Pontin, 2014; Craig & Sneyd, 2005; Longbottom et al., 1998; Wilmot-Smith et al., 2009a,b).

* yaozhou@princeton.edu

Pontin et al. (2009) has later found that its current density output can violate charge conservation, and mimetic discretization has been applied to fix it (Candelaresi et al., 2014).

Recently, a variational integrator for ideal MHD in Lagrangian labeling has been developed by Zhou et al. (2014) using discrete exterior calculus (Desbrun et al., 2005). Derived in a geometric and field-theoretic manner, it naturally preserves many of the conservation laws of ideal MHD, including charge conservation. It is arguably an optimal tool for studying current singularity formation.

Zhou et al. (2016) have used this method to study the Hahm-Kulsrud-Taylor (HKT) problem (Hahm & Kulsrud, 1985), a fundamental prototype problem for current singularity formation in 2D, where a plasma in a sheared magnetic field is subject to boundary forcing. The formation of current singularity is conclusively confirmed via convergence study, and its signature is also identified in other 2D cases with more complex topology, such as the coalescence instability of magnetic islands (Longcope & Strauss, 1993).

In this paper, we extend the HKT problem to 3D line-tied geometry. Zweibel & Li (1987) showed that the linear solution, which is singular in 2D, should become smooth. This prediction is confirmed by our numerical results. However, we also find that given finite amplitude, the linear solution can be pathological when the system is sufficiently long. We speculate that this finite-amplitude pathology may trigger a finite-length singularity in the nonlinear solution.

We perform convergence study on the nonlinear solutions for varying system length L. For short systems, the nonlinear solutions converge to smooth ones. The peak current density approximately scales with $(L_n - L)^{-1}$, suggesting that the solution may become singular above a finite length L_n. However, the solutions for longer systems inherently involve strongly sheared motions, which often lead to mesh distortion in our numerical method. As a result, we cannot obtain solutions for systems with lengths close to L_n, and hence cannot conclude whether such a finite-length singularity does exist. Nonetheless, our results are suggestive that current singularity may well survive in this line-tied system, in accordance with the arguments in Ng & Bhattacharjee (1998).

This paper is organized as follows. In Sec. II we formulate the Parker problem in Lagrangian labeling, specify the setup in line-tied geometry, and introduce the conventions of reduced MHD. Our numerical method is illustrated in Sec. III. In Sec. IV we review the conclusions from the HKT problem in 2D, and then present our results, both linear and nonlinear, in 3D line-tied geometry. Discussions follow in Sec. V.

II. THE PARKER PROBLEM

Parker (1972) originally considered a perfectly conducting plasma magnetized by a uniform field $\mathbf{B} = \hat{z}$ threaded between two planes at $z = 0, L$, which are often referred to as footpoints. The footpoints are then subject to random motions such that the magnetic field becomes nonuniform. He argued that in general, there exists no smooth equilibrium for the system to relax to, and therefore current singularities must form. This conjecture is based on perturbative analysis of the magnetostatic equilibrium equation,

$$(\nabla \times \mathbf{B}) \times \mathbf{B} = \nabla p, \tag{1}$$

where p is the pressure. Many of the subsequent works on the Parker problem are performed on this equation as well (Antiochos, 1987; Bogoyavlenskij, 2000; Janse et al., 2010; Low, 2006, 2010; Parker, 1983; Rosner & Knobloch, 1982; Tsinganos et al., 1984; van Ballegooijen, 1985).

A caveat of this approach is that Eq. (1) is usually underdetermined. That is, a given set of boundary conditions may allow for more than one solution to this equation, and additional information is needed to identify a specific one. Often it is prescribed to the equilibrium, such as the pressure and guide field profiles in the Grad-Shafranov equation (Grad, 1967). For the Parker problem, the information is the very constraint to preserve the initial magnetic topology. The implication is, identifying singular solutions to Eq. (1) does not necessarily prove Parker's conjecture, since these solutions may not be topologically constrained.

However, this topological constraint is mathematically challenging to explicitly attach to Eq. (1) and its solutions (Janse et al., 2010; Low, 2010). Nonetheless, it can be naturally enforced if one adopts Lagrangian labeling for ideal MHD, instead of Eulerian labeling that is used in Eq. (1), as first noticed by Zweibel & Li (1987).

A. Lagrangian labeling

In Lagrangian labeling, the motion of the fluid elements is traced in terms of a continuous mapping from the initial position $\mathbf{x}_0$ to the current position $\mathbf{x}(\mathbf{x}_0, t)$. In this formulation, the advection (continuity, adiabatic, and frozen-in) equations are (Newcomb, 1962)

$$\rho\, \mathrm{d}^3x = \rho_0\, \mathrm{d}^3x_0 \Rightarrow \rho = \rho_0/J, \tag{2a}$$

$$p/\rho^\gamma = p_0/\rho_0^\gamma \Rightarrow p = p_0/J^\gamma, \tag{2b}$$

$$B_i\, \mathrm{d}S_i = B_{0i}\, \mathrm{d}S_{0i} \Rightarrow B_i = x_{ij}B_{0j}/J, \tag{2c}$$

where $x_{ij} = \partial x_i/\partial x_{0j}$, $J = \det(x_{ij})$ is the Jacobian, γ the adiabatic index, $\rho_0 = \rho(\mathbf{x}_0, 0)$ the initial mass density, and the same goes for p_0 and $\mathbf{B}_0$. They reflect the fact that in ideal MHD, mass, entropy, and magnetic flux are advected by the motion of the fluid elements. They are built into the ideal MHD Lagrangian and the subsequent Euler-Lagrange equation (Newcomb, 1962),

$$\rho_0\ddot{x}_i - B_{0j}\frac{\partial}{\partial x_{0j}}\left(\frac{x_{ik}B_{0k}}{J}\right) + \frac{\partial J}{\partial x_{ij}}\frac{\partial}{\partial x_{0j}}\left(\frac{p_0}{J^\gamma} + \frac{x_{kl}x_{km}B_{0l}B_{0m}}{2J^2}\right) = 0. \quad (3)$$

This is the momentum equation, the only ideal MHD equation in Lagrangian labeling.

Without time dependence, Eq. (3) becomes an equilibrium equation. Its solutions will satisfy not only Eq. (1) but automatically the topological constraint implied in the Parker problem, since the initial field configuration $\mathbf{B}_0$ is built into the equation. In contrast, not all solutions to Eq. (1) can necessarily be mapped from given initial conditions.

Thus, the equilibrium equation in Lagrangian labeling offers a more natural and mathematically explicit description for the Parker problem, which simply becomes whether there exist singular solutions to such equation, given certain smooth initial and boundary conditions. If the initial field $\mathbf{B}_0$ is smooth, any singularity in the equilibrium field $\mathbf{B}$ should trace back to that in the fluid mapping $\mathbf{x}(\mathbf{x}_0)$. In Sec. II.B, we will specify the initial and boundary conditions for the Parker problem.

B. 3D line-tied geometry

Parker's original model can be characterized with a uniform initial field $\mathbf{B}_0 = \hat{z}$ and prescribed smooth footpoint motion $\mathbf{x}_\perp(\mathbf{x}_{0\perp})$ at $z_0 = 0, L$ while $z|_{z_0=0,L} = z_0$. The subscript $\perp$ denotes the in-plane components (x, y). Certain classes of footpoint motion were considered in Craig & Sneyd (2005); Longbottom et al. (1998); Mikić et al. (1989); Ng & Bhattacharjee (1998); van Ballegooijen (1988), which are referred to as braiding experiments in the recent review by Wilmot-Smith (2015).

An alternative is to consider a nonuniform $\mathbf{B}_0$, referred to as initially braided field in Wilmot-Smith (2015), with no-slip footpoints ($\mathbf{x} = \mathbf{x}_0$ at $z_0 = 0, L$). Note that to remain relevant to Parker's original model, the nonuniform $\mathbf{B}_0$ must be realizable from the Parker's uniform field via smooth footpoint motion. Examples include the coalescence instability (Longcope & Strauss, 1994a,b) and the threaded X-point (Craig & Pontin, 2014), but exclude those with magnetic nulls (Craig & Effenberger, 2014; Pontin & Craig, 2005).

We adopt the latter approach for its two advantages. One is reduced computational complexity. More importantly, these initially braided fields are usually extended from 2D cases that are susceptible to current singularity formation (Craig & Litvinenko, 2005; Longcope & Strauss, 1993). Unlike Parker's original setup, this allows one to focus on the effect of 3D line-tied geometry on current singularity formation. In Sec. IV, we will extend the HKT problem (Hahm & Kulsrud, 1985), where current singularity formation is confirmed in 2D (Zhou et al., 2016), to 3D line-tied geometry.

C. Reduced MHD

Reduced MHD (RMHD, Strauss, 1976) is an approximation of MHD in the strong guide field limit that is often used to model the solar corona. van Ballegooijen (1985) first used what essentially is RMHD to study the Parker problem.

In Eulerian labeling, RMHD approximations include uniform guide field ($B_z = 1$), removal of z dynamics ($v_z = 0$), and incompressibility ($\nabla \cdot \mathbf{v} = 0$). The equilibrium equation becomes

$$\mathbf{B} \cdot \nabla j_z = 0, \quad (4)$$

which is the z component of the curl of Eq. (1). Here $\mathbf{j} = \nabla \times \mathbf{B}$ is the current density.

Physically, Eq. (4) means that j_z is constant along a field line. In RMHD, every field line is threaded through all z. Therefore, the implication for the Parker problem is, if an equilibrium solution yields current singularity, it must penetrate into the line-tied boundaries. Note that this is a very strong condition that applies to all solutions of Eq. (4), topologically constrained or not.

Translated into Lagrangian labeling, RMHD approximations become $B_{0z} = 1$, $z = z_0$, and $J = 1$. Following Eq. (2c), the in-plane field now reads

$$\mathbf{B}_\perp = \frac{\partial \mathbf{x}_\perp}{\partial \mathbf{x}_{0\perp}} \cdot \mathbf{B}_{0\perp} + \frac{\partial \mathbf{x}_\perp}{\partial z_0}. \quad (5)$$

The first term on the RHS results from in-plane motion, while the second term is the projection of the tilted guide field that shows up only in 3D.

At the line-tied boundaries ($z_0 = 0, L$), where $\mathbf{x}_\perp = \mathbf{x}_{0\perp}$, the z component of the (Eulerian) curl of Eq. (5) reads

$$j_z\hat{z} = j_{0z}\hat{z} + \nabla_\perp \times \frac{\partial \mathbf{x}_\perp}{\partial z_0}. \quad (6)$$

Here j_{0z} is the initial condition that has to be smooth. That is, for j_z to be (nearly) singular at the footpoints, $(\partial\mathbf{x}_\perp/\partial z_0)|_{z_0=0,L}$ must be (nearly) singularly sheared (note that this is compatible with the line-tied boundary condition). Therefore, we assert that strongly sheared motion is an inherent feature of the Parker problem.

Throughout the rest of the paper, RMHD approximations are adopted unless otherwise noted. We comment that the boundary layers close to the footpoints that are identified in full MHD analysis (Scheper & Hassam, 1999; Zweibel & Boozer, 1985; Zweibel & Li, 1987) are precluded in RHMD, which makes current singularity formation even more difficult. Nonetheless, we expect that if a current singularity can emerge in RMHD, it will likely survive in full MHD.

III. NUMERICAL METHOD

Numerically, many have used Eulerian methods for ideal MHD to study the Parker problem (Longcope & Strauss, 1994a; Mikić et al., 1989; Ng & Bhattacharjee, 1998; Rappazzo & Parker, 2013). These simulations all end up encountering artificial reconnection, and topologically constrained equilibrium solutions cannot be obtained.

In contrast, Lagrangian methods that solve Eq. (3) with moving meshes avoid solving the frozen-in equation and the subsequent artificial reconnection. For example, a Lagrangian relaxation scheme (Craig & Sneyd, 1986) has been extensively used to study the Parker problem (Craig & Pontin, 2014; Craig & Sneyd, 2005; Longbottom et al., 1998; Wilmot-Smith et al., 2009a,b). In this method, the inertia (first term) in Eq. (3) is replaced by frictional damping, which has been argued to cause unphysical artifacts by (Low, 2013). Also, Pontin et al. (2009) showed that the spatial discretization using conventional finite difference can violate charge conservation ($\nabla\cdot\mathbf{j}=0$). Both of these issues have been fixed in Candelaresi et al. (2014): the former by keeping the inertia during the relaxation, and the latter with mimetic discretization.

The numerical method we use is a recently developed variational integrator for ideal MHD (Zhou et al., 2014). It is obtained by discretizing the Lagrangian for ideal MHD in Lagrangian labeling (Newcomb, 1962) on a moving unstructured mesh. Using discrete exterior calculus (Desbrun et al., 2005), the momentum equation (3) is spatially discretized into a conservative many-body form $M_i\ddot{\mathbf{x}}_i = -\partial V/\partial\mathbf{x}_i$, where M_i and $\mathbf{x}_i$ are the mass and position of the ith vertex, respectively, and V is a spatially discretized potential energy. When the system is integrated in time, friction may be introduced to dynamically relax it to an equilibrium with minimal V.

Compared with similar methods (Candelaresi et al., 2014; Craig & Sneyd, 1986), our method exactly preserves many conservation laws including charge conservation. Our discrete force is conservative, which means the equilibrium solution minimizes a discrete potential energy. Constructed on unstructured meshes, the method allows resolution to be devoted to where it is most needed, such as the vicinity of a potential current singularity.

An Achilles' heel of our numerical method, and others that solve Eq. (3) with moving meshes, is its vulnerability to mesh distortion due to strong shear flow. Unfortunately, as discussed in Sec. II.C, strongly sheared motion is an inherent nature of the Parker problem, posing a formidable challenge for our numerical endeavor at the very outset.

IV. THE HKT PROBLEM

The HKT problem was originally proposed by Taylor and studied by Hahm & Kulsrud (1985), in the context of studying forced magnetic reconnection induced by resonant perturbation on a rational surface. It considers a 2D incompressible plasma in a sheared equilibrium field $B_{0y} = x_0$. The perfectly conducting boundaries at $x_0 = \pm a$ are subject to sinusoidal perturbations so that $x(\pm a, y_0) = \pm[a - \delta\cos ky(\pm a, y_0)]$.

Zweibel & Li (1987) first connected this problem to the Parker problem, since the sheared initial field is easily realizable from Parker's uniform field via sheared footpoint motion. In 2D, Their linear equilibrium solution in Lagrangian labeling reads

$$\chi = -\frac{\delta a \sinh kx_0 \sin ky_0}{k|x_0|\sinh ka}. \tag{7}$$

where χ is the stream function for the linear displacement $\boldsymbol{\xi} = \nabla\chi\times\hat{z}$. Note that the linear equilibrium equation in Lagrangian labeling is simply $\mathbf{F}(\boldsymbol{\xi}) = 0$, where $\mathbf{F}$ is the ideal MHD force operator (Schnack, 2009).

The linear solution (7) yields a current singularity at the neutral line $x_0 = 0$, resulting from the singularity in $\partial\xi_x/\partial x_0$. Nonetheless, such a normal discontinuity in the displacement is not physically permissible (see Fig. 3 and relevant discussion in Sec. IV.B). The failure at the neutral line is expected from the linear solution since the linear assumption breaks down there.

It has remained unclear whether the nonlinear solution to this problem is singular, until Zhou et al. (2016) used the numerical method described in Sec. III to confirm it. It is found that the equilibrium fluid mapping normal to the neutral line at $y_0 = 0$, namely $x(x_0, 0)$, converges to a quadratic power law $x \sim x_0^2$. Due to incompressibility, $(\partial y/\partial y_0)|_{y_0=0} \sim x_0^{-1}$ diverges at $x_0 = 0$. With the sheared initial field $B_{0y} = x_0$ substituted into Eq. (5), such a mapping leads to an equilibrium field $B_y \sim \mathrm{sgn}(x)$ that is discontinuous at the neutral line.

Physically, this means the fluid element at the origin $(0, 0)$ is infinitely compressed normally towards, while infinitely stretched tangentially along the neutral line. The exact same signature of current singularity is also identified in other 2D cases with more complex topology, such as the coalescence instability of magnetic islands (Longcope & Strauss, 1993). It appears to be a general recipe for current singularity formation in 2D, which we shall refer to as "squashing" in this article.

The question then becomes whether squashing works in 3D line-tied geometry. We can learn from Eq. (5) that squashing is 2D in-plane motion that only contributes to the first term on the RHS. At the footpoints, where in-plane motion is absent and Eq. (6) holds, squashing does not work anymore. Hence, we expect 3D line-tied geometry to have a smoothing effect on the 2D current singularity. Yet we need to find out whether it eliminates the singularity entirely.

A. Linear results

For the HKT problem in 2D, the singularity in the linear solution appears to be very suggestive for that in the nonlinear solution. Naturally, when extending the problem to 3D line-tied geometry, we consider the linear solution first.

In 3D line-tied geometry, we modulate the boundary forcing at $x_0 = \pm a$ into the form of $x(\pm a, y_0, z_0) = \pm[a - \delta \cos ky(\pm a, y_0, z_0)\sin(\pi z_0/L)]$. The perturbations vanish at the footpoints ($z_0 = 0, L$), consistent with the line-tied (no-slip) boundary condition. Accounting for the initial field $B_{0y} = x_0$, adopting RMHD conventions ($B_{0z} = 1$ and $\boldsymbol{\xi} = \nabla\chi \times \hat{z}$) and Fourier dependence $\chi = \bar{\chi}(x_0, z_0)\exp iky_0$, the linear equilibrium equation $\mathbf{F}(\boldsymbol{\xi}) = 0$ becomes

$$(ikx_0 + \partial_{z_0})(\partial^2_{x_0} - k^2)(ikx_0 + \partial_{z_0})\bar{\chi} = 0. \qquad (8)$$

When $\partial_{z_0} = 0$, the 2D solution (7) can be recovered.

Eq. (8) is solved using 2nd-order finite difference, with boundary conditions $\bar{\chi}|_{x_0=\pm a} = \pm i(\delta/k)\sin(\pi z_0/L)$ and $\bar{\chi}|_{z_0=0,L} = 0$. The parameters used are $a = 0.25$, $k = 2\pi$, $\delta = 0.05$, with varying L and resolution $N \times NL/8$. For a given L, the numerical solutions are found to converge to a smooth one. In Fig. 1, $\xi_x(x_0, 0, L/2)$ obtained with different resolutions for $L = 32$ are shown to converge.

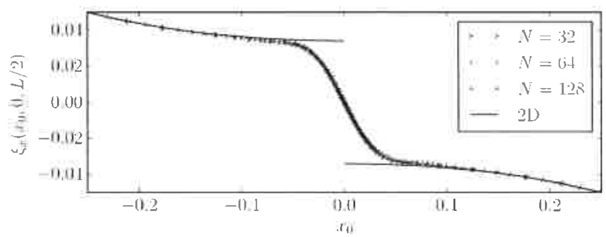

FIG. 1 Numerical solutions of $\xi_x(x_0, 0, L/2)$ for $L = 32$ with $N = 32$, 64, and 128 converge. Solid line shows the 2D solution (7).

We also find that with increasing L, $\xi_x(x_0, 0, L/2)$ approaches the 2D solution with discontinuity (solid line in Fig. 1). Accordingly, the maximum of the linearly calculated current density $j_{0z} + \delta j_z$, where $j_{0z} = 1$ and δj_z is the perturbed current density, is shown to increase linearly with L in Fig. 2 (labeled j_l). This suggests that the linear solution is smooth for arbitrary L, only becoming singular when $L = \infty$. These results are consistent with the 3D linear analysis by Zweibel & Li (1987).

It is worthwhile to emphasize that so far all the calculations have been strictly linear, assuming the amplitude

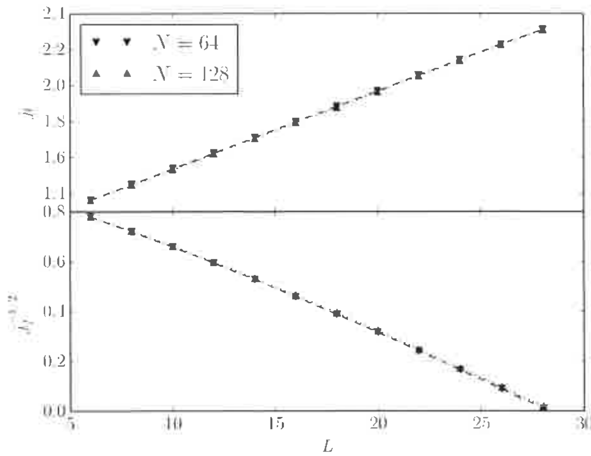

FIG. 2 Maximum of the linearly calculated current density j_l (top), and inverse square root of the maximum of the finite-amplitude current density j_f (bottom, see Sec. IV.B), vs. system length L for $N = 64$ and 128. j_l increases linearly with L, while $j_f \sim (L_f - L)^{-2}$ can roughly be observed.

of the perturbation δ to be infinitesimal. The linear solutions, be they ξ_x or δj_z, are proportional to δ. The magnitude of δ has no physical impact in this context.

The finite amplitude of the perturbation must be accounted for in the fully nonlinear study. But before that, we further exploit the linear solutions by considering the effect of finite amplitude on them in Sec. IV.B.

B. Finite-amplitude pathology

Now consider fluid mapping $\mathbf{x} = \mathbf{x}_0 + \boldsymbol{\xi}$, where $\boldsymbol{\xi}$ is the linear equilibrium displacement with finite amplitude δ. $\mathbf{x}$ is by no means a nonlinear equilibrium solution. That is, it does not satisfy the nonlinear equilibrium equation in Lagrangian labeling [Eq. (3) without time dependence]. Nonetheless, one can still calculate "nonlinearly" the magnetic field it maps into, using Eq. (2c), and the current density j_z thereafter, which we refer to as the finite-amplitude current density in this paper.

We perform such calculation using the linear solutions obtained (with $\delta = 0.05$) in Sec. IV.A, and notice that the finite-amplitude current density peaks at $(0, 0, L/2)$. As shown in Fig. 2, the maximum $j_f \sim (L_f - L)^{-2}$, which diverges at a critical length L_f. The value $L_f \approx 28.96$ (using solutions with $N = 128$ for fitting) depends on the specific parameters we obtain the linear solutions with, δ in particular.

When $L > L_f$, $\mathbf{x}$ becomes pathological, its Jacobian J no longer everywhere positive. More specifically, one finds $x(x_0, 0, L/2)$ to be non-monotonic: $\partial x/\partial x_0 < 0$, or equivalently, $\partial\xi_x/\partial x_0 < -1$, at $(0, 0, L/2)$. Physically, this means the flux surfaces (constant surfaces of flux function $\psi_0 = x_0^2/2$) overlap, as illustrated in Fig. 3.

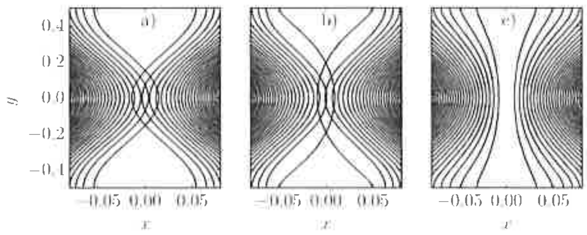

FIG. 3 Contours of flux function subject to perturbation with $\delta = 0.05$: 2D solution (7) (a), and 3D solutions at the mid-plane for $L = 64$ (b) and $L = 16$ (c). The intersection of contours in (a) and (b) are pathological.

Note that this pathology is also the reason the discontinuity in the linear solution in 2D (7) is not physically permissible, which is shown in Fig. 3 as well. The difference is, in 2D, $\partial\xi_x/\partial x_0$ is singular, so the pathology exists for infinitesimal amplitude; while in 3D, $\partial\xi_x/\partial x_0$ is smooth, and finite amplitude is required to trigger the pathology at a critical length.

Recall that $\partial x/\partial x_0 = 0$, the trigger for the pathology, is also a signature of current singularity that is identified in the 2D HKT problem. Interestingly, Loizu et al. (2015) have also linked similar finite-amplitude pathology of the linear solution to the existence of current singularity in 3D equilibria. We therefore suspect that the nonlinear solution to the line-tied HKT problem may be singular above a finite length, which is presumably comparable to the critical length L_f for the finite-amplitude pathology of the linear solution. Also, we expect the maximum current density of the nonlinear solution to be bounded between j_l and j_f. We investigate whether our nonlinear results support these speculations in Sec. IV.C.

C. Nonlinear results

We solve the line-tied HKT problem numerically using the method described in Sec. III, in a domain of $[-a, a] \times [-\pi/k, \pi/k] \times [0, L]$. At $x_0 = \pm a$ it is constrained that $x = \pm[a - \delta\cos ky\sin(\pi z/L)]$. The boundary conditions in y and z are periodic and no-slip, respectively. We use the same parameters as used in the linear study, namely $a = 0.25$, $k = 2\pi$, $\delta = 0.05$, with varying L.

In addition, we adopt RMHD approximations that is described in Sec. II.C, by setting $B_{0z} = 1$ and $z = z_0$. For the sake of numerical practicality, we use moderate pressure to approximate incompressibility, instead of enforcing the constraint $J = 1$. After all, incompressibility itself is an approximation. Specifically, we initialize with $p_0 = 0.1 - x_0^2/2$ to balance the sheared field $B_{0y} = x_0$, and choose $\gamma = 5/3$. In our numerical solutions, we find $|J - 1| \lesssim 0.02$.

A consequence of approximating $J = 1$ is that Eq. (4) does not hold anymore, but instead we have $\mathbf{B}\cdot\nabla j_z = \mathbf{j}\cdot\nabla B_z$ with $B_z = 1/J$. Since the system is symmetric under rotation by π with respect to the z axis ($x, y = 0$, the field line of interest in this problem), one finds that $\mathbf{B}_\perp = \mathbf{j}_\perp = 0$, and therefore $j_z(z) = j_z(0)/J(z)$, along the z axis. So in our solutions $j_z(0,0,z)$ should still be approximately constant.

We use a tetrahedral mesh where the vertices are arranged in a structured manner with resolution $N \times 2N \times NL/4$. The grid number in z varies with L so that the grid size does not. The vertices are non-uniformly distributed in x and y to devote more resolution near the z axis. We use a same profile of mesh packing for a given L, but adjust it accordingly when L varies.

The system starts from a smoothly perturbed configuration consistent with the boundary conditions and relax to equilibrium. In Fig. 4, the equilibrium current density distributions obtained with $N = 160$ for $L = 6$, 12, and 18 are shown. Despite that the distributions become significantly more concentrated to the z axis with increasing L, all these solutions turn out to be smooth and well-resolved, as our convergence study shows.

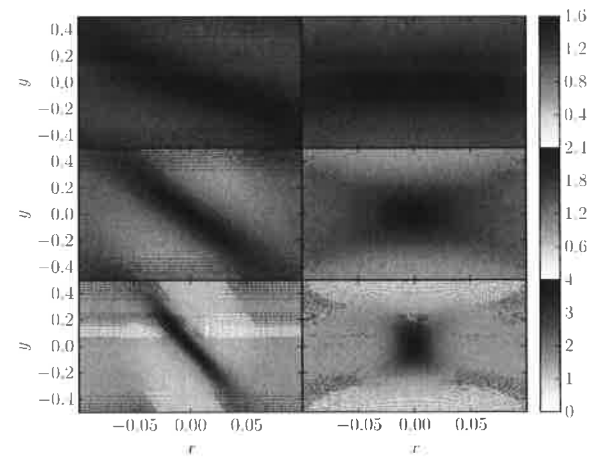

FIG. 4 Distribution of current density $j_z(x, y)$ obtained with $N = 160$ for $L = 6$, 12, and 18 (from top to bottom, respectively) at $z = 0$ (left) and $z = L/2$ (right).

In Fig. 5, the means of $j_z(0, 0, z)$ (labeled j_n) for varying L are shown to converge with increasing resolution N. In addition, the standard deviations of $j_z(0, 0, z)$, as shown by the error bars, decrease with increasing N. That is, $j_z(0, 0, z)$ is indeed approximately constant, as predicted. We therefore conclude that the nonlinear solutions for these relatively short systems are smooth.

Another observation from Fig. 5 is that the standard deviation of $j_z(0, 0, z)$ increases with L. The reason is, for longer systems, the footpoints are more difficult to resolve than the mid-plane. At the footpoints, there is no in-plane motion, which means the mesh there stays as initially prescribed. Meanwhile, as L increases, the mid-plane bears more resemblance with the 2D case, where

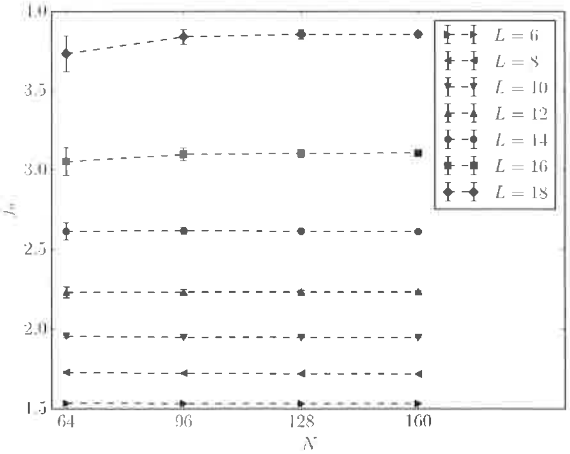

FIG. 5 The means (j_n) and the standard deviations (error bars) of the current density $j_z(0,0,z)$ for varying system length L are shown to converge with incresing resolution N.

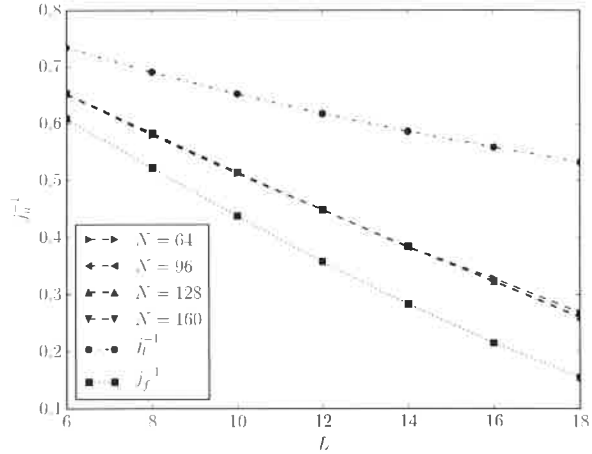

FIG. 6 Inverse of the mean (j_n) of the current density $j_z(0,0,z)$ (dashed lines) with varying resolution N vs. system length L. $j_n \sim (L_n - L)^{-1}$ can roughly be observed. j_l (dash-dot line) and j_f (dotted line) are also shown for comparison (solutions with $N = 128$ from Fig. 2 are used).

the squashing effect spontaneously packs the mesh near the z axis. In fact, in the simulations, we need to pack the mesh more aggressively near the footpoints than the mid-plane, particularly for longer systems, in order to compensate for the self-packing near the mid-plane. To sum up, longer systems are simply much more challenging to resolve computationally than shorter ones.

Fig. 6 shows that j_n^{-1} decreases roughly linearly with L. That is, $j_n \sim (L_n - L)^{-1}$, which diverges at a critical length L_n. This suggests that the nonlinear solution may become singular at a finite length. Using the solutions with $N = 160$ for fitting, we obtain $L_n \approx 25.81$, which is comparable to the critical length L_f for the finite-amplitude pathology discussed in Sec. IV.B. Fig. 6 also shows that j_n is indeed bounded between j_l and j_f, as expected.

In order to validate such a diverging scaling law and confirm the existence of the finite-length singularity, we should examine the solutions for systems with lengths close to or above the critical value L_n. Unfortunately, we are not able to obtain (converged) equilibrium solutions for systems with $L = 20$ or higher: as $j_z(0,0,z)$ increases with L, the motion near the footpoints becomes more strongly sheared, eventually leading to mesh distortion, as discussed in Secs. II.C and III. As L increases, $j_z(0,0,z)$ may indeed diverge at a finite length, or convert to a different scaling law that stays well-defined for arbitrary L. With the results in hand, we cannot confirm or rule out either possibility conclusively.

V. DISCUSSION

One conclusion we can indeed draw from our results is that 3D line-tied geometry does have a smoothing effect on the current singularity in the 2D HKT problem. In 2D, both linear and nonlinear solutions yield a current singularity. In 3D line-tied geometry, the linear solution is smooth for all system lengths; the nonlinear solution is smooth when the system is short.

Whether the nonlinear solution becomes singular at a finite length remains yet to be confirmed. Our numerical results show that the maximum current density scales with $(L_n - L)^{-1}$, which implies finite-length singularity. However, since we cannot obtain numerical solutions to validate such a scaling law near the critical value L_n, these results can only be considered suggestive, but not conclusive. Nonetheless, we remark that this scaling law is already stronger than the exponential scaling that is predicted by Longcope & Strauss (1994b).

In this paper, we have prescribed what we believe is an effective formula for realizing possible current singularities in 3D line-tied geometry. The idea is to extend a 2D case with singularity to 3D line-tied geometry, and then make the system really long. In particular, the HKT problem is arguably a simplest prototype, for it captures how a sheared field responds to squashing, both ingredients ubiquitous in nature. Also, the finite-amplitude pathology in its linear solution may be suggestive for the possible finite-length singularity in the nonlinear solution.

The results of the HKT problem can also be suggestive for other cases with more complex magnetic topology, such as the internal kink instability (Huang et al., 2006; Rosenbluth et al., 1973) and the coalescence instability (Longcope & Strauss, 1993, 1994a,b). The obvious distinction between the HKT problem and these cases is the former is externally forced, while the latter are instability driven. A subtlety is, for the instability driven cases, the linear equilibrium equation $\mathbf{F}(\boldsymbol{\xi}) = 0$ usually has no nontrivial solutions. In these cases, (fastest-growing) eigenmodes are usually considered to as linear solutions. In addition, eigenmodes do not have intrinsic amplitudes, unlike in the HKT problem where the linear equilibrium solution can reasonably be given the finite amplitude of the boundary forcing. Consequently, the linear solutions in the instability driven cases can be less suggestive for the nonlinear ones.

Nonetheless, critical lengths still exist in 3D line-tied geometry for the instability driven cases. That is, these systems are unstable only with lengths above certain finite values (Huang et al., 2006; Longcope & Strauss, 1994a,b). In fact, Ng & Bhattacharjee (1998) argued that current singularities must emerge when the line-tied systems become unstable.

Still, what prevents us from obtaining more conclusive results is the limitation of our numerical method, namely its vulnerability to mesh distortion caused by strongly sheared motion. There are a few remedies that are worth investigating. One option is to enforce incompressibility ($J = 1$), since the signature of mesh distortion is J becoming negative. However, naively enforcing this constraint means implicitly solving a global nonlinear equation at every time step, which is not practical. What might make things better is to solve for pressure from a Poisson-like equation, yet that could still be expensive on an unstructured mesh. More importantly, when the motion becomes too strongly sheared for the mesh to resolve, enforcing incompressibility may just not be enough.

An alternative is to employ adaptive mesh refinement. Intuitively, that means to divide a simplex into smaller ones once its deformation reaches a certain threshold. This approach will not work for problems with strong background shear flows where the number of simplices can grow exponentially, but may suffice for the Parker problem that is quasi-static. In addition, one may consider more delicate discretization of Eq. (3) to make the mesh itself more robust against shear flow.

Finally, we emphasize that the Parker problem is still open and of practical relevance, by echoing the latest review by Zweibel & Yamada (2016): *"It is important to determine whether the equilibrium of line-tied magnetic fields has true current singularities or merely very large and intermittent currents, to characterize the statistical properties of the sheets and to determine how the equilibrium level and spatial and temporal intermittency of energy release depend on S."*

ACKNOWLEDGMENTS

We thank E. G. Zweibel for helpful discussions and comments on an early version of this manuscript. This research was supported by the U.S. Department of Energy under Contract No. DE-AC02-09CH11466, and used resources of the Oak Ridge Leadership Computing Facility at the Oak Ridge National Laboratory, which is supported by the Office of Science of the U.S. Department of Energy under Contract No. DE-AC05-00OR22725.

REFERENCES

Antiochos, S. K. 1987, The Astrophysical Journal, 312, 886
Bogoyavlenskij, O. I. 2000, Physical Review Letters, 84, 1914
Candelaresi, S., Pontin, D. I., & Hornig, G. 2014, SIAM Journal on Scientific Computing, 36, 15
—. 2015, The Astrophysical Journal, 808, 134
Craig, I. J. D., & Effenberger, F. 2014, The Astrophysical Journal, 795, 129
Craig, I. J. D., & Litvinenko, Y. E. 2005, Physics of Plasmas, 12, 032301
Craig, I. J. D., & Pontin, D. I. 2014, The Astrophysical Journal, 788, 177
Craig, I. J. D., & Sneyd, A. D. 1986, The Astrophysical Journal, 311, 451
—. 2005, Solar Physics, 232, 41
Desbrun, M., Hirani, A. N., Leok, M., & Marsden, J. E. 2005, arXiv preprint math/0508.341, arXiv:0508.341
Grad, H. 1967, Physics of Fluids, 10, 137
Hahm, T. S., & Kulsrud, R. M. 1985, Physics of Fluids, 28, 2412
Huang, Y.-M., Zweibel, E. G., & Sovinec, C. R. 2006, Physics of Plasmas, 13, 092102
Janse, Å. M., Low, B. C., & Parker, E. N. 2010, Physics of Plasmas, 17, 092901
Loizu, J., Hudson, S. R., Bhattacharjee, A., Lazerson, S., & Helander, P. 2015, Physics of Plasmas, 22, 090704
Longbottom, A. W., Rickard, G. J., Craig, I. J. D., & Sneyd, A. D. 1998, The Astrophysical Journal, 500, 471
Longcope, D. W., & Strauss, H. R. 1993, Physics of Fluids B: Plasma Physics, 5, 2858
—. 1994a, The Astrophysical Journal, 426, 742
—. 1994b, The Astrophysical Journal, 437, 851
Low, B. C. 2006, The Astrophysical Journal, 649, 1064
—. 2010, The Astrophysical Journal, 718, 717
—. 2013, The Astrophysical Journal, 768, 7
Mikić, Z., Schnack, D. D., & van Hoven, G. 1989, The Astrophysical Journal, 338, 1148
Newcomb, W. A. 1962, Nuclear Fusion: Supplement, part 2, 2, 451
Ng, C. S., & Bhattacharjee, A. 1998, Physics of Plasmas, 5, 4028
Parker, E. N. 1972, The Astrophysical Journal, 174, 499
—. 1983, The Astrophysical Journal, 264, 635
—. 1994, Spontaneous current sheets in magnetic fields: with applications to stellar x-rays, Vol. 1 (New York: Oxford University Press)
Pontin, D. I., Candelaresi, S., Russell, A. J. B., & Hornig, G. 2016, Plasma Physics and Controlled Fusion, 58, 054008
Pontin, D. I., & Craig, I. J. D. 2005, Physics of Plasmas, 12, 072112
Pontin, D. I., & Hornig, G. 2015, The Astrophysical Journal, 805, 47
Pontin, D. I., Hornig, G., Wilmot-Smith, A. L., & Craig, I. J. D. 2009, The Astrophysical Journal, 700, 1449
Rappazzo, A. F., & Parker, E. N. 2013, The Astrophysical Journal Letters, 773, L2

Rosenbluth, M. N., Dagazian, R. Y., & Rutherford, P. H. 1973, Physics of Fluids, 16, 1894

Rosner, R., & Knobloch, E. 1982, The Astrophysical Journal, 262, 349

Scheper, R. A., & Hassam, A. B. 1999, The Astrophysical Journal, 511, 976

Schnack, D. D. 2009, in Lectures in Magnetohydrodynamics (Springer), 77–83

Strauss, H. R. 1976, Physics of Fluids, 19, 134

Tsinganos, K. C., Rosner, R., & Distler, J. 1984, The Astrophysical Journal, 278, 409

van Ballegooijen, A. A. 1985, The Astrophysical Journal, 298, 421

—. 1988, Geophysical & Astrophysical Fluid Dynamics, 41, 181

Wilmot-Smith, A. L. 2015, Philosophical Transactions of the Royal Society A: Mathematical, Physical and Engineering Sciences, 373, 20140265

Wilmot-Smith, A. L., Hornig, G., & Pontin, D. I. 2009a, The Astrophysical Journal, 696, 1339

—. 2009b, The Astrophysical Journal, 704, 1288

Zhou, Y., Huang, Y.-M., Qin, H., & Bhattacharjee, A. 2016, Physical Review E, 93, 023205

Zhou, Y., Qin, H., Burby, J. W., & Bhattacharjee, A. 2014, Physics of Plasmas, 21, 102109

Zweibel, E. G., & Boozer, A. H. 1985, The Astrophysical Journal, 295, 642

Zweibel, E. G., & Li, H.-S. 1987, The Astrophysical Journal, 312, 423

Zweibel, E. G., & Yamada, M. 2016, Proceedings of the Royal Society A: Mathematical, Physical and Engineering Science, 472, 20160479

Antiochos, S. K. 1987, The Astrophysical Journal, 312, 886

Bogoyavlenskij, O. I. 2000, Physical Review Letters, 84, 1914

Candelaresi, S., Pontin, D. I., & Hornig, G. 2014, SIAM Journal on Scientific Computing, 36, 15

—. 2015, The Astrophysical Journal, 808, 134

Craig, I. J. D., & Effenberger, F. 2014, The Astrophysical Journal, 795, 129

Craig, I. J. D., & Litvinenko, Y. E. 2005, Physics of Plasmas, 12, 032301

Craig, I. J. D., & Pontin, D. I. 2014, The Astrophysical Journal, 788, 177

Craig, I. J. D., & Sneyd, A. D. 1986, The Astrophysical Journal, 311, 451

—. 2005, Solar Physics, 232, 41

Desbrun, M., Hirani, A. N., Leok, M., & Marsden, J. E. 2005, arXiv preprint math/0508.341, arXiv:0508.341

Grad, H. 1967, Physics of Fluids, 10, 137

Hahm, T. S., & Kulsrud, R. M. 1985, Physics of Fluids, 28, 2412

Huang, Y.-M., Zweibel, E. G., & Sovinec, C. R. 2006, Physics of Plasmas, 13, 092102

Janse, Å. M., Low, B. C., & Parker, E. N. 2010, Physics of Plasmas, 17, 092901

Loizu, J., Hudson, S. R., Bhattacharjee, A., Lazerson, S., & Helander, P. 2015, Physics of Plasmas, 22, 090704

Longbottom, A. W., Rickard, G. J., Craig, I. J. D., & Sneyd, A. D. 1998, The Astrophysical Journal, 500, 471

Longcope, D. W., & Strauss, H. R. 1993, Physics of Fluids B: Plasma Physics, 5, 2858

—. 1994a, The Astrophysical Journal, 426, 742

—. 1994b, The Astrophysical Journal, 437, 851

Low, B. C. 2006, The Astrophysical Journal, 649, 1064

—. 2010, The Astrophysical Journal, 718, 717

—. 2013, The Astrophysical Journal, 768, 7

Mikić, Z., Schnack, D. D., & van Hoven, G. 1989, The Astrophysical Journal, 338, 1148

Newcomb, W. A. 1962, Nuclear Fusion: Supplement, part 2, 2, 451

Ng, C. S., & Bhattacharjee, A. 1998, Physics of Plasmas, 5, 4028

Parker, E. N. 1972, The Astrophysical Journal, 174, 499

—. 1983, The Astrophysical Journal, 264, 635

—. 1994, Spontaneous current sheets in magnetic fields: with applications to stellar x-rays. Vol. 1 (New York: Oxford University Press)

Pontin, D. I., Candelaresi, S., Russell, A. J. B., & Hornig, G. 2016, Plasma Physics and Controlled Fusion, 58, 054008

Pontin, D. I., & Craig, I. J. D. 2005, Physics of Plasmas, 12, 072112

Pontin, D. I., & Hornig, G. 2015, The Astrophysical Journal, 805, 47

Pontin, D. I., Hornig, G., Wilmot-Smith, A. L., & Craig, I. J. D. 2009, The Astrophysical Journal, 700, 1449

Rappazzo, A. F., & Parker, E. N. 2013, The Astrophysical Journal Letters, 773, L2

Rosenbluth, M. N., Dagazian, R. Y., & Rutherford, P. H. 1973, Physics of Fluids, 16, 1894

Rosner, R., & Knobloch, E. 1982, The Astrophysical Journal, 262, 349

Scheper, R. A., & Hassam, A. B. 1999, The Astrophysical Journal, 511, 976

Schnack, D. D. 2009, in Lectures in Magnetohydrodynamics (Springer), 77–83

Strauss, H. R. 1976, Physics of Fluids, 19, 134

Tsinganos, K. C., Rosner, R., & Distler, J. 1984, The Astrophysical Journal, 278, 409

van Ballegooijen, A. A. 1985, The Astrophysical Journal, 298, 421

—. 1988, Geophysical & Astrophysical Fluid Dynamics, 41, 181

Wilmot-Smith, A. L. 2015, Philosophical Transactions of the Royal Society A: Mathematical, Physical and Engineering Sciences, 373, 20140265

Wilmot-Smith, A. L., Hornig, G., & Pontin, D. I. 2009a, The Astrophysical Journal, 696, 1339

—. 2009b, The Astrophysical Journal, 704, 1288

Zhou, Y., Huang, Y.-M., Qin, H., & Bhattacharjee, A. 2016, Physical Review E, 93, 023205

Zhou, Y., Qin, H., Burby, J. W., & Bhattacharjee, A. 2014, Physics of Plasmas, 21, 102109

Zweibel, E. G., & Boozer, A. H. 1985, The Astrophysical Journal, 295, 642

Zweibel, E. G., & Li, H.-S. 1987, The Astrophysical Journal, 312, 423

Zweibel, E. G., & Yamada, M. 2016, Proceedings of the Royal Society A: Mathematical, Physical and Engineering Science, 472, 20160479